



Regulation of inorganic carbon acquisition in a red tide alga (*Skeletonema costatum*): the importance of phosphorus availability

Guang Gao^{a,b}, Jianrong Xia^{a*}, Jinlan Yu^a, Jiale Fan^b, Xiaopeng Zeng^a

^aSchool of Environmental Science and Engineering, Guangzhou University, Guangzhou, 510006, China

^bMarine Resources Development Institute of Jiangsu, Huaihai Institute of Technology, Lianyungang, 222005, China

*Corresponding author, Email: jrxia@gzhu.edu.cn; Phone: +86 (0)20 39366941; Fax: +86 (0)20 39366949



1 **Abstract:**

2 *S. costatum* is a common bloom-forming diatom and encounters eutrophication and severe
3 CO₂ limitation during red tides. However, little is known regarding the role of phosphorus in
4 modulating inorganic carbon acquisition in *S. costatum*, particularly under CO₂ limitation
5 conditions. We cultured *S. costatum* under five phosphate levels (0.05, 0.25, 1, 4, 10 μmol L⁻¹)
6 and then treated it with two CO₂ conditions (2.8 and 12.6 μmol L⁻¹) for two hours. The lower
7 CO₂ reduced net photosynthetic rate at lower phosphate levels (< 4 μmol L⁻¹) but did not
8 affect it at higher phosphate levels (4 and 10 μmol L⁻¹). In contrast, the lower CO₂ induced
9 higher dark respiration rate at lower phosphate levels (0.05 and 0.25 μmol L⁻¹) and did not
10 affect it at higher phosphate levels (> 1 μmol L⁻¹). The lower CO₂ did not change rETR at
11 lower phosphate levels (0.05 and 0.25 μmol L⁻¹) and increased it at higher phosphate levels (>
12 1 μmol L⁻¹). Photosynthetic CO₂ affinity ($K_{0.5}$) decreased with phosphate levels. The lower
13 CO₂ did not affect $K_{0.5}$ at 0.05 μmol L⁻¹ phosphate but reduced it at the other phosphate levels.
14 Activity of extracellular carbonic anhydrase was dramatically induced by the lower CO₂ at
15 phosphate replete conditions (> 0.25 μmol L⁻¹) and the same pattern also occurred for redox
16 activity of plasma membrane. Direct HCO₃⁻ use was induced when phosphate concentration is
17 more than 1 μmol L⁻¹. This study indicates the essential role of P in regulating inorganic
18 carbon acquisition and CO₂ concentrating mechanisms (CCMs) in *S. costatum* and sheds light
19 on how bloom-forming algae cope with carbon limitation during the development of red tides.

20 **Keywords:** carbonic anhydrase; CO₂ concentrating mechanisms; pH compensation point;
21 photosynthesis; redox activity; respiration



22 1. Introduction

23 Diatoms are unicellular photosynthetic microalgae that can be found worldwide in
24 freshwater and oceans. Marine diatoms account for 75% of the primary productivity for
25 coastal and other nutrient-rich zones and approximately 20% of global primary production
26 (Field *et al.*, 1998; Falkowski, 2012), hence playing a vital role in marine biological carbon
27 pump as well as the biogeochemical cycling of important nutrients, such as nitrogen and
28 silicon (Nelson *et al.*, 1995; Moore *et al.*, 2013; Young & Morel, 2015). Diatoms usually
29 dominate the phytoplankton communities and form large-scale blooms in nutrient-rich zones
30 and upwelling regions (Bruland *et al.*, 2001; Anderson *et al.*, 2008; Barton *et al.*, 2016).
31 Nutrient enrichment is considered as a compelling factor that triggers algal blooms albeit the
32 occurrence of diatom blooms may be modulated by other environmental factors, such as
33 temperature, light intensity, salinity etc. (Smetacek & Zingone, 2013; Jeong *et al.*, 2015).
34 When inorganic nitrogen and phosphorus are replete, diatoms could out-compete
35 chrysophytes, raphidophytes and dinoflagellates (Berg *et al.*, 1997; Jeong *et al.*, 2015; Barton
36 *et al.*, 2016) and dominate algal blooms due to their quicker nutrient uptake and growth rate.

37 In normal natural seawater (pH 8.1, salinity 35), HCO_3^- is the majority (~90%) of total
38 dissolved inorganic carbon (DIC, 2.0–2.2 mM). CO_2 (1%, 10–15 μM), which is the only
39 direct carbon source that can be assimilated by all photosynthetic organisms, only accounts
40 for 1% of total dissolved inorganic carbon. Diatoms' ribulose-1,5-bisphosphate
41 carboxylase/oxygenase (RUBISCO) has a relatively low affinity for CO_2 and is commonly
42 less than half saturated under current CO_2 levels in seawater (Hopkinson & Morel, 2011),
43 suggesting that CO_2 is limited for marine diatoms' carbon fixation. To cope with the CO_2



4

44 limitation in seawater and maintain a high carbon fixation rate under the low CO₂ conditions,
45 diatoms have evolved various inorganic carbon acquisition pathways and CO₂ concentrating
46 mechanisms, for instance, active transport of HCO₃⁻, the passive influx of CO₂, multiple
47 carbon anhydrase, assumed C4-type pathway, etc. (Hopkinson & Morel, 2011; Hopkinson *et*
48 *al.*, 2016). *S. costatum* is a worldwide diatom species that can be found from equatorial to
49 polar waters. It usually dominates large-scale algal blooms in eutrophic seawaters (Wang,
50 2002; Li *et al.*, 2011). When blooms occur, seawater pH increases and CO₂ decreases. For
51 instance, pH level in the surface waters of the eutrophic Mariager Fjord, Denmark, could be
52 up to 9.75 during algal blooms (Hansen, 2002). Consequently, *S. costatum* experiences very
53 severe CO₂ limitation when blooms occur. To deal with it, *S. costatum* has developed multiple
54 CCMs (Nimer *et al.*, 1998; Rost *et al.*, 2003). However, contrasting findings were reported.
55 Nimer *et al.* (1998) documented that extracellular carbonic anhydrase activity in *S. costatum*
56 was only induced when CO₂ concentration was less than 5 μmol L⁻¹ while Rost *et al.* (2003)
57 reported that activity of extracellular CA could be detected even when pCO₂ is 1800 μatm.
58 Chen and Gao (2004) showed that in *S. costatum* had little capacity in direct HCO₃⁻ utilization.
59 On the other hand, Rost *et al.* (2003) demonstrated that this species could take up CO₂ and
60 HCO₃⁻ simultaneously.

61 Phosphorus (P) is an indispensable element for all living organisms, serving as an integral
62 component of lipids, nucleic acids, ATP and a diverse range of other metabolites. Levels of
63 bioavailable phosphorus are very low in many ocean environments and phosphorus
64 enrichment can commonly increase algal growth and marine primary productivity in the
65 worldwide oceans (Davies & Sleep, 1989; Müller & Mitrovic, 2015; Lin *et al.*, 2016). Due to



66 the essential role of phosphorus, extensive studies have been conducted to investigate the
67 effect of phosphorus on photosynthetic performances (Geider *et al.*, 1998; Liu *et al.*, 2012;
68 Beamud *et al.*, 2016), growth (Jiang *et al.*, 2016; Reed *et al.*, 2016; Mccall *et al.*, 2017),
69 phosphorus acquisition, utilization and storage (Lin *et al.*, 2016 and the references therein).
70 Some studies show the relationship between phosphorus availability and inorganic carbon
71 acquisition in green algae (Beardall *et al.*, 2005; Hu & Zhou, 2010). In terms of *S. costatum*,
72 studies regarding the inorganic carbon acquisition in *S. costatum* focus on its response to
73 variation of CO₂ availability. The role of phosphorus in *S. costatum*'s CCMs remains
74 unknown. Based on the connection between phosphorus and carbon metabolism in diatoms
75 (Brembu *et al.*, 2017), we hypothesize that phosphorus enrichment could enhance the capacity
76 of inorganic carbon utilization and hence maintain high rates of photosynthesis and growth in
77 *S. costatum* under CO₂ limitation conditions. In the present study, we investigated the
78 inorganic acquisition pathways, photosynthetic CO₂ affinity, carbonic anhydrase activity,
79 redox activity of plasma membrane, and photosynthetic rate under five levels of phosphate
80 and two levels of CO₂ conditions to test this hypothesis. Our study would provide helpful
81 insights into how bloom-forming diatoms overcome CO₂ limitation to maintain a quick
82 growth rate during red tides.

83 2. Materials and Methods

84 2.1. Culture conditions

85 *S. costatum* (Grev.) Cleve from Jinan University, China, was cultured in f/2 artificial
86 seawater with five phosphate levels (0.05, 0.25, 1, 4, 10 μmol L⁻¹) by adding different
87 amounts of NaH₂PO₄ 2H₂O. The cultures were carried out semi-continuously at 20°C for



88 seven days. The light irradiance was set $200 \mu\text{mol m}^{-2} \text{s}^{-1}$, with a light and dark period of 12:
89 12. The cultures were aerated with ambient air (0.3 L min^{-1}) to maintain the pH around 8.2.
90 The cells during exponential phase were collected and rinsed twice with DIC-free seawater
91 that was made according to Xu *et al.* (2017). Afterwards, cells were resuspended in fresh
92 media with two levels of pH (8.2 and 8.7, respectively corresponding to ambient CO_2 (12.6
93 $\mu\text{mol L}^{-1}$, AC) and low CO_2 ($2.8 \mu\text{mol L}^{-1}$, LC) under corresponding phosphate levels for two
94 hours before the following measurements, with a cell density of $1.0 \times 10^6 \text{ mL}^{-1}$. This transfer
95 aimed to investigate the effects of phosphate on DIC acquisition under a CO_2 limitation
96 condition. The pH of 8.7 was chosen considering that it is commonly used as a CO_2 limitation
97 condition (Nimer *et al.*, 1998; Chen & Gao, 2004) and also occurs during algal bloom
98 (Hansen, 2002). Two hours should be enough to activate CCMs in *S. costatum* (Nimer *et al.*,
99 1998). All experiments were conducted in triplicates.

100 2.2. Chlorophyll fluorescence measurement

101 Chlorophyll fluorescence was measured with a pulse modulation fluorometer
102 (PAM-2100, Walz, Germany). The measuring light and actinic light were 0.01 and $200 \mu\text{mol}$
103 $\text{photons m}^{-2} \text{s}^{-1}$, respectively. The saturating pulse was set $4,000 \mu\text{mol photons m}^{-2} \text{s}^{-1}$ (0.8 s).
104 Relative electron transport (rETR, $\mu\text{mol e}^- \text{m}^{-2} \text{s}^{-1}$) = $(F_M' - F_t) / F_M' \times 0.5 \times \text{PFD}$, where F_M'
105 is the maximal fluorescence levels from algae after in light, F_t is the fluorescence at an
106 excitation level and PFD is the actinic light density.

107 2.3. Estimation of photosynthetic oxygen evolution and respiration

108 The net photosynthetic rate and respiration rate of *S. costatum* were measured using a
109 Clark-type oxygen electrode (YSI Model 5300, USA) that was held in a circulating water bath



7

110 (Cooling Circulator; Cole Parmer, Chicago, IL, USA) to keep the setting temperature (20°C).
111 Five mL of samples were transferred to the oxygen electrode cuvette and were stirred during
112 measurement. The light intensity and temperature were maintained as the same as that in the
113 growth condition. The illumination was provided by a halogen lamp. The increase of oxygen
114 content in seawater within five minutes was defined as net photosynthetic rate. To measure
115 dark respiration rate, the samples were placed in darkness and the decrease of oxygen content
116 within ten minutes was defined as dark respiration rate. Net photosynthetic rate and dark
117 respiration rate were presented as $\mu\text{mol O}_2 (10^9 \text{ cells})^{-1} \text{ h}^{-1}$.

118 To obtain the curve of net photosynthetic rate versus DIC, seven levels of DIC (0, 0.1, 0.2,
119 0.5, 1, 2, and 4 mM) were made by adding different amounts of NaHCO_3 to the Tris buffered
120 DIC-free seawater. The algal samples were washed twice with DIC-free seawater before
121 transferring to the various DIC solutions. Photosynthetic rates at different DIC levels were
122 measured under saturating irradiance of $400 \mu\text{mol photons m}^{-2} \text{ s}^{-1}$ and growth temperature.
123 The algal samples were allowed to equilibrate for 2–3 min at each DIC level during which
124 period a linear change in oxygen concentration was obtained and recorded. The parameter,
125 photosynthetic half saturation constant ($K_{0.5}$, i.e., the DIC concentration required to give half
126 of C_i -saturated maximum rate of photosynthetic O_2 evolution), was calculated from the
127 Michaelis-Menten kinetics equation (Caemmerer and Farquhar 1981): $V = V_{max} \times [S] / (K_{0.5} +$
128 $[S])$, where V is the real-time photosynthetic rate, V_{max} is maximum photosynthetic rate and $[S]$
129 is the DIC concentration. $K_{0.5}$ for CO_2 was calculated via CO2SYS (Pierrot *et al.*, 2006),
130 using the equilibrium constants of K_1 and K_2 for carbonic acid dissociation (Roy *et al.*, 1993)
131 and the KSO_4^- dissociation constant from Dickson (1990). Total alkalinity and pH were the



132 two input parameters. Seawater pH was measured with a pH meter (pH 700, Eutech
133 Instruments, Singapore) and total alkalinity was measured by titrations.

134 2.4. Measurement of photosynthetic pigment

135 To determine the photosynthetic pigment (Chl *a*) content, 50 mL of culture were filtered
136 on a Whatman GF/F filter, extracted in 5 mL of 90% acetone for 12 h at 4°C, and centrifuged
137 (3, 000 g, 5 min). The optical density of the supernatant was scanned from 200 to 700 nm
138 with a UV-VIS spectrophotometer (Shimadzu UV-1800, Kyoto, Japan). The concentration of
139 Chl *a* was calculated based on the optical density at 630 and 664 nm: $\text{Chl } a = 11.47 \times \text{OD}_{664} -$
140 $0.40 \times \text{OD}_{630}$, $\text{Chl } c = 24.36 \times \text{OD}_{630} - 3.73 \times \text{OD}_{664}$.

141 2.5. Measurement of extracellular carbonic anhydrase activity

142 Carbonic anhydrase activity was assessed using the electrometric method (Gao *et al.*,
143 2009). Cells were harvested by centrifugation at 4, 000 g for five minutes at 20°C, washed
144 once and resuspended in 8 mL Na-barbital buffer (20 mM, pH 8.2). Five mL CO₂-saturated
145 icy distilled water was injected into the cell suspension, and the time required for a pH
146 decrease from 8.2 to 7.2 at 4°C was recorded. Extracellular carbonic anhydrase (CA_{ext})
147 activity was measured using intact cells. CA activity (E.U.) was calculated using the
148 following formula: $\text{E.U.} = 10 \times (\text{T}_0 / \text{T} - 1)$, where T₀ and T represent the time required for the
149 pH change in the absence or presence of the samples, respectively.

150 2.6. Measurement of redox activity in the plasma membrane

151 The redox activity of plasma membrane was assayed by incubating the cells with 500
152 μmol ferricyanide [K₃Fe(CN)₆] that cannot penetrate intact cells and has been used as an
153 external electron acceptor (Nimer *et al.*, 1998; Wu & Gao, 2009). Stock solutions of



154 $\text{K}_3\text{Fe}(\text{CN})_6$ were freshly prepared before use. Five mL of samples were taken after two hours
155 of incubation and centrifuged at 4000 g for 10 min (20°C). The absorbance of supernatant at
156 420 nm was measured immediately to assess the rate of exofacial ferricyanide reduction
157 (Nimer et al., 1998).

158 2.7. pH drift experiment

159 To obtain the pH compensation point, the cells were transferred to sealed glass vials
160 containing fresh medium (pH 8.2) with corresponding phosphate levels. The cell
161 concentration for all treatments was $5.0 \times 10^5 \text{ mL}^{-1}$. The pH drift of the suspension was
162 monitored at 20°C and 200 $\mu\text{mol photons m}^{-2} \text{ s}^{-1}$ light level. The pH compensation point was
163 obtained when there was no a further increase in pH.

164 2.8. Statistical analysis

165 Results were expressed as means of replicates \pm standard deviation and data were
166 analyzed using the software SPSS v.21. The data from each treatment conformed to a normal
167 distribution (Shapiro-Wilk, $P > 0.05$) and the variances could be considered equal (Levene's
168 test, $P > 0.05$). Two-way ANOVAs were conducted to assess the effects of CO_2 and phosphate
169 on differences net photosynthetic rate, dark respiration rate, ratio of net photosynthetic rate to
170 dark respiration rate, rETR, Chl *a*, $K_{0.5}$, CA_{ext} , reduction rate of ferricyanide, and pH
171 compensation point. Least Significant Difference (LSD) was conducted for *post hoc*
172 investigation. Repeated measures ANOVAs were conducted to analyze the effects of DIC on
173 net photosynthetic rate and the effect of incubation time on media pH in a closed system.
174 Bonferroni was conducted for *post hoc* investigation. The threshold value for determining
175 statistical significance was $P < 0.05$.



176 3. Results

177 3.1. Effects of CO₂ and phosphate on photosynthetic and respiratory performances

178 The net photosynthetic rate and dark respiration rate in *S. costatum* grown at various CO₂
179 and phosphate concentrations were first investigated (Fig. 1). CO₂ interacted with phosphate
180 on net photosynthetic rate ($F_{(4, 20)} = 3.662$, $P = 0.021$, Fig. 1a), with each factor having a main
181 effect ($F_{(1, 20)} = 11.286$, $P = 0.003$ for CO₂, $F_{(4, 20)} = 157.925$, $P < 0.001$ for phosphate). *Post*
182 *hoc* LSD comparison ($P = 0.05$) showed that LC reduced net photosynthetic rate when the
183 phosphate levels was below 4 $\mu\text{mol L}^{-1}$ but did not affect it at the higher phosphate levels.
184 Under AC, net photosynthetic rate increased with phosphate level and reached the plateau at 1
185 $\mu\text{mol L}^{-1}$ phosphate. Under LC, net photosynthetic rate also increased with phosphate level
186 but did not hit the peak until 4 $\mu\text{mol L}^{-1}$ phosphate. Phosphate had a main effect on dark
187 respiration rate ($F_{(4, 20)} = 169.050$, $P < 0.001$, Fig. 1b), and it interacted with CO₂ ($F_{(4, 20)} =$
188 3.226 , $P = 0.034$). Specifically, LC increased dark respiration rate at 0.05 and 0.25 $\mu\text{mol L}^{-1}$
189 phosphate levels, but did not affect it when phosphate level was above 1 $\mu\text{mol L}^{-1}$ (LSD, $P <$
190 0.05). Regardless of CO₂ level, respiration rate increased with phosphate availability and
191 stopped at 1 $\mu\text{mol L}^{-1}$.

192 The ratio of respiration to photosynthesis ranged from 0.23 to 0.40 (Fig. 2). Both CO₂ and
193 phosphate had a main effect ($F_{(1, 20)} = 32.443$, $P < 0.001$ for CO₂, $F_{(4, 20)} = 7.081$, $P = 0.001$ for
194 phosphate), and they interplayed on the ratio of respiration to photosynthesis ($F_{(4, 20)} = 8.299$,
195 $P < 0.001$). LC increased the ratio when phosphate was lower than 4 $\mu\text{mol L}^{-1}$ but did not
196 affect it when phosphate levels were 4 or 10 $\mu\text{mol L}^{-1}$.

197



198 Both CO₂ and phosphate affected rETR ($F_{(1, 20)} = 28.717$, $P < 0.001$ for CO₂, $F_{(4, 20)} =$
199 127.860 , $P < 0.001$ for phosphate) and they also showed an interactive effect ($F_{(4, 20)} = 3.296$,
200 $P = 0.031$, Fig. 3). For instance, *post hoc* LSD comparison showed that LC did not affect
201 rETR at lower phosphate levels (0.05 and 0.25 $\mu\text{mol L}^{-1}$) but increased it at higher phosphate
202 levels (1–10 $\mu\text{mol L}^{-1}$). Regardless of CO₂ treatment, rETR increased with phosphate level
203 (0.05–4 $\mu\text{mol L}^{-1}$) but the highest phosphate concentration did not result in a further increase
204 in rETR (LSD, $P = 0.05$).

205 The content of Chl *a* was measured to investigate the effects of CO₂ and phosphate on
206 photosynthetic pigment in *S. costatum* (Fig. 4). Both CO₂ and phosphate affected the
207 synthesis of Chl *a* ($F_{(1, 20)} = 32.963$, $P < 0.001$ for CO₂, $F_{(4, 20)} = 92.045$ $P < 0.001$ for
208 phosphate) and they had an interactive effect ($F_{(4, 20)} = 3.871$, $P = 0.017$). *Post hoc* LSD
209 comparison ($P = 0.05$) showed that LC did not affect Chl *a* at 0.05 or 0.25 $\mu\text{mol L}^{-1}$ phosphate
210 but stimulated Chl *a* synthesis at higher phosphate levels (1–10 $\mu\text{mol L}^{-1}$). Irrespective of CO₂
211 treatment, Chl *a* content increased with phosphate level and reached the plateau at 4 $\mu\text{mol L}^{-1}$
212 phosphate.

213 To access the effects of CO₂ and phosphate on photosynthetic CO₂ affinity in *S. costatum*,
214 the net photosynthetic rates of cells exposure to seven levels of DIC were measured (Fig. 5).
215 After curve fitting, the values of $K_{0.5}$ for CO₂ were calculated (Fig. 6). CO₂ and phosphate
216 interplayed on $K_{0.5}$ ($F_{(4, 20)} = 3.821$, $P = 0.018$) and each had a main effect ($F_{(1, 20)} = 96.182$, P
217 < 0.001 for CO₂, $F_{(4, 20)} = 40.497$, $P < 0.001$ for phosphate). LC did not affect $K_{0.5}$ at the
218 lowest phosphate level but reduced it at the other phosphate levels. Under AC, higher
219 phosphate levels (0.25–4 $\mu\text{mol L}^{-1}$) reduced $K_{0.5}$ and the highest phosphate level led to a



220 further decrease in $K_{0.5}$ compared to $0.05 \mu\text{mol L}^{-1}$ phosphate. The pattern with phosphate
221 under LC was the same as the AC.

222 3.3. The effects of CO_2 and phosphate on inorganic carbon acquisition

223 To investigate the potential mechanisms that cells overcame CO_2 limitation during algal
224 blooms, the activity of CA_{ext} , a CCM related enzyme, was estimated under various CO_2 and
225 phosphate conditions (Fig. 7a). Both CO_2 ($F_{(1, 20)} = 569.585$, $P < 0.001$) and phosphate ($F_{(4, 20)}$
226 $= 176.392$, $P < 0.001$) had a main effect and they interacted ($F_{(4, 20)} = 87.380$, $P < 0.001$) on
227 CA_{ext} activity. *Post hoc* LSD comparison ($P = 0.05$) showed that LC induced more CA_{ext}
228 activity under all phosphate conditions except for $0.05 \mu\text{mol L}^{-1}$ levels, compared to AC.
229 Under AC, CA_{ext} activity increased with phosphate level and stopped increasing at $1 \mu\text{mol L}^{-1}$
230 phosphate. Under LC, CA_{ext} activity also increased with phosphate level but reached the peak
231 at $4 \mu\text{mol L}^{-1}$ phosphate. The redox activity of plasma membrane was also assayed to
232 investigate the factors that modulate CA_{ext} activity (Fig. 7b). The pattern of redox activity of
233 plasma membrane under various CO_2 and phosphate conditions was the same as that of CA_{ext}
234 activity. That is, CO_2 and phosphate had an interactive effect ($F_{(4, 20)} = 137.050$, $P < 0.001$) on
235 redox activity of plasma membrane, each having a main effect ($F_{(1, 20)} = 937.963$, $P < 0.001$
236 for CO_2 ; $F_{(4, 20)} = 276.362$, $P < 0.001$ for phosphate).

237 To test cells' tolerance to high pH and obtain pH compensation points in *S. costatum*
238 grown under various CO_2 and phosphate levels, changes of media pH in a closed system were
239 monitored (Fig. 8). The media pH under all phosphate conditions increased with incubation
240 time ($F_{(10, 100)} = 7604.563$, $P < 0.001$). Specifically speaking, there was a steep increase in pH
241 during the first three hours, afterwards the increase became slower and it reached a plateau in



242 six hours (Bonferroni, $P < 0.05$). Phosphate had an interactive effect with incubation time
243 ($F_{(10, 100)} = 47.469$, $P < 0.001$). For instance, there was no significant difference in media pH
244 among phosphate levels during first two hours of incubation but then divergence occurred and
245 they stopped at different points. Two-way ANOVA analysis showed that CO₂ treatment did
246 not affect pH compensation point ($F_{(1, 20)} = 0.056$, $P = 0.816$) but phosphate had a main effect
247 ($F_{(4, 20)} = 226.196$, $P < 0.001$). Under each CO₂ treatment, pH compensation point increased
248 with phosphate level, with lowest of 9.03 ± 0.03 at $0.05 \mu\text{mol L}^{-1}$ and highest of 9.36 ± 0.04 at
249 $10 \mu\text{mol L}^{-1}$ phosphate.

250 4. Discussion

251 4.1. Photosynthetic performances under various CO₂ and phosphate conditions

252 The lower CO₂ availability reduced the net photosynthetic rate of *S. costatum* grown at
253 the lower phosphate levels in the present study. However, Nimer *et al.* (1998) demonstrated
254 that the increase in pH (8.3–9.5) did not reduce photosynthetic CO₂ fixation of *S. costatum*
255 and Chen and Gao (2004) reported that a higher pH (8.7) even stimulated the photosynthetic
256 rate of *S. costatum* compared to the control (pH 8.2). The divergence between our and the
257 previous studies may be due to different nutrient supply. Both Nimer *et al.* (1998) and Chen
258 and Gao (2004) used f/2 media to grow algae. The phosphate concentration in f/2 media is
259 $\sim 36 \mu\text{mol L}^{-1}$, which is replete for physiological activities in *S. costatum*. *S. costatum* grown
260 at higher phosphate levels (4 and $10 \mu\text{mol L}^{-1}$) also showed comparative photosynthetic rates
261 between the lower and higher CO₂ treatments. Our finding combined with the previous
262 studies indicates phosphorus plays an important role in dealing with low CO₂ availability for
263 photosynthesis in *S. costatum*.



264 Different from net photosynthetic rate, LC did not affect rETR at lower phosphate levels
265 (0.05 and 0.25 $\mu\text{mol L}^{-1}$) and stimulated it at higher phosphate levels (1–10 $\mu\text{mol L}^{-1}$). This
266 interactive effect of CO_2 and phosphate may be due to their effects on Chl *a*. LC induced
267 more synthesis of Chl *a* at higher phosphate levels (1–10 $\mu\text{mol L}^{-1}$). This induction of LC on
268 photosynthetic pigment is also reported in green algae (Gao *et al.*, 2016). More energy is
269 required under LC to address the more severe CO_2 limitation and thus more Chl *a* are
270 synthesized to capture more light energy, particularly when phosphate was replete. Although P
271 is not an integral component for chlorophyll, it plays an important role in cell energetics
272 through high-energy phosphate bonds, i.e. ATP, which could support chlorophyll synthesis.
273 The stimulating effect of P enrichment on photosynthetic pigment is also found in green alga
274 *Dunaliella tertiolecta* (Geider *et al.*, 1998) and brown alga *Sargassum muticum* (Xu *et al.*,
275 2017). The increased photosynthetic pigment in *S. costatum* could partially explain the
276 increased rETR and photosynthetic rate under the higher P conditions.

277 4.2. Ratio of respiration to photosynthesis

278 The ratio of respiration to photosynthesis in algae indicates carbon balance in cells and
279 carbon flux in marine ecosystems as well (Zou & Gao, 2013). LC increased this ratio in *S.*
280 *costatum* grown at the lower P conditions but did not affect it under the higher P conditions,
281 indicating that P enrichment can offset the carbon loss caused by carbon limitation. To cope
282 with CO_2 limitation, cells might have to obtain energy from dark respiration under lower P
283 conditions as it seems infeasible to acquire energy from the low rETR, which led to the
284 increased dark respiration. However, LC induced higher rETR under P replete conditions and
285 energy used for inorganic carbon acquisition could be from the increased rETR. Therefore,



286 additional dark respiration was not triggered, avoiding carbon loss. Most studies regarding the
287 effect of CO₂ on ratio of respiration to photosynthesis focus on higher plants (Gifford, 1995;
288 Ziska & Bunce, 1998; Cheng *et al.*, 2010; Smith & Dukes, 2013), little is known on
289 phytoplankton. Our study suggests that CO₂ limitation may lead to carbon loss in
290 phytoplankton but P enrichment could alter this trend, regulating carbon balance in
291 phytoplankton and thus their capacity in carbon sequestration.

292 4.3. Inorganic carbon acquisition under CO₂ limitation and phosphate enrichment

293 Decreased CO₂ can usually induce higher inorganic carbon affinity in algae (Raven *et al.*,
294 2012; Wu *et al.*, 2012; Raven *et al.*, 2017; Xu *et al.*, 2017). In the present study, the lower
295 CO₂ did increase inorganic carbon affinity when P level was higher than 0.25 μmol L⁻¹ but did
296 not affect it when P was 0.05 μmol L⁻¹, indicating the important role of P in regulating cells'
297 CCMs in response to environmental CO₂ changes. LC induced larger CA activity when P was
298 above 0.25 μmol L⁻¹ but did not increase it at 0.05 μmol L⁻¹ of P, which could explain the
299 interactive effect of P and CO₂ on inorganic carbon affinity as CA can accelerate the
300 equilibrium between HCO₃⁻ and CO₂ and increase inorganic carbon affinity. Regardless of
301 CO₂, P enrichment alone increased CA activity and inorganic carbon affinity. P enrichment
302 may stimulate the synthesis of CA by supplying required ATP. In addition, P enrichment
303 increased redox activity of plasma membrane in this study. It has been proposed that redox
304 activity of plasma membrane could induce eextracellular CA activity via protonation
305 extrusion of its active center (Nimer *et al.*, 1998). Our result that the pattern of CA is exactly
306 same as that of redox activity of plasma membrane shows a compelling correlation between
307 CA and redox activity of plasma membrane. The stimulating effect of P on redox activity of



308 plasma membrane may be due to its effect on rETR. The increased rETR could generate
309 excess reducing equivalents, particularly under CO₂ limited conditions. These excess reducing
310 equivalents would be transported from the chloroplast into the cytosol (Heber, 1974),
311 supporting the redox chain in the plasma membrane (Rubinstein & Luster, 1993; Nimer *et al.*,
312 1999) and triggering CA activity.

313 4.4. Direct HCO₃⁻ utilization due to phosphate enrichment

314 A pH compensation point over 9.2 has been considered a sign of direct HCO₃⁻ use for
315 algae (Axelsson & Uusitalo, 1988) as CO₂ concentration is nearly zero at pH above 9.2. This
316 criterion has been justified based on the experiments for both micro and macro-algae. For
317 instance, the marine diatom *Phaeodactylum tricornutum*, with strong capacity for direct
318 HCO₃⁻ utilization, has a higher pH compensation point of 10.3 (Chen *et al.*, 2006). In contrast,
319 red macroalgae, *Lomentaria articulata* and *Phycodryis rubens* that cannot utilize HCO₃⁻
320 directly and photosynthesis only depends on CO₂ diffusion, have pH compensation points of
321 less than 9.2 (Maberly, 1990). In terms of *S. costatum*, it has been reported to have a pH
322 compensation point of 9.12, indicating a very weak capacity in direct HCO₃⁻ utilization (Chen
323 & Gao, 2004). Our study demonstrates that the pH compensation point of *S. costatum* varies
324 with the availability of P. It is lower than 9.2 under P limiting conditions but higher than 9.2
325 under P replete conditions, suggesting that the capacity of direct HCO₃⁻ utilization is regulated
326 by P availability. Contrary to CO₂ passive diffusion, the direct use of HCO₃⁻ depends on
327 positive transport that requires energy (Hopkinson & Morel, 2011). P enrichment increased
328 rETR in the present study and the ATP produced during the process of electron transport could
329 be used to support HCO₃⁻ positive transport. In addition, the increased respiration at higher P



330 levels can also generate ATP to help HCO_3^- positive transport. Our study indicates that P
331 enrichment could trigger HCO_3^- direct utilization and hence increase inorganic acquisition
332 capacity of *S. costatum* to cope with CO_2 limitation.

333 4.5. CCMs and red tides

334 With the development of red tides, the pH in seawater could be very high along with
335 extremely low CO_2 availability due to intensive photosynthesis (Hansen, 2002; Hinga, 2002).
336 For instance, pH level in the surface waters of the eutrophic Mariager Fjord, Denmark, is
337 often above 9 during dinoflagellate blooms (Hansen, 2002). Diatoms are the casautive species
338 for red tides and *S. costatum* could outcompete other bloom algae (dinoflagellates
339 *Prorocentrum minimum* and *Alexandrium tamarense*) under nutrient replete conditions (Hu *et*
340 *al.*, 2011). However, potential mechanisms are poorly understood. Our study demonstrates *S.*
341 *costatum* has multiple CCMs to cope with CO_2 limitation and the operation of CCMs is
342 regulated by P availability. The CCMs of *S. costatum* is hampered under P limiting conditions
343 and only function when P is replete. Therefore, P enrichment would be critical for *S. costatum*
344 to overcome carbon limitation during algal bloom and to dominate red tides.

345 5. Conclusions

346 The present study investigated the role of P in regulating inorganic carbon acquisition and
347 CO_2 concentrating mechanisms in diatoms for the first time. The intensive photosynthesis and
348 quick grow during algal blooms usually result in noticeable increase of pH and decrease of
349 CO_2 . Our study demonstrates that P enrichment could induce activity of extracellular carbonic
350 anhydrase and direct utilization of HCO_3^- in *S. costatum* to help overcome the CO_2 limitation,
351 as well as increasing photosynthetic pigment content and rETR to provide required energy.



352 This study provides important insight into the connection of phosphorus and carbon
353 acquisition in diatoms and the mechanisms that *S. costatum* dominates algal blooms.

354 **Author contribution**

355 JX and GG designed the experiments, and GG, JY, JF and XZ carried them out. GG
356 prepared the manuscript with contributions from all co-authors.

357 **Acknowledgements**

358 This work was supported by National Natural Science Foundation of China (No.
359 41376156 & 40976078), Natural Science Fund of Guangdong Province (No.
360 S2012010009853), Science and Technology Bureau of Lianyungang (SH1606), Jiangsu
361 Planned Projects for Postdoctoral Research Funds (1701003A), Science Foundation of
362 Huaihai Institute of Technology (Z2016007), and
363 Foundation for High-level Talents in Higher Education of Guangdong.

364 **References**

365 **Anderson DM, Burkholder JM, Cochlan WP, Glibert PM, Gobler CJ, Heil CA, Kudela**

366 **R, Parsons ML, Rensel JE, Townsend DW. 2008.** Harmful algal blooms and
367 eutrophication: Examining linkages from selected coastal regions of the United States.
368 *Harmful Algae* **8**: 39-53.

369 **Axelsson L, Uusitalo J. 1988.** Carbon acquisition strategies for marine macroalgae. *Marine*
370 *Biology* **97**: 295-300.

371 **Barton AD, Irwin AJ, Finkel ZV, Stock CA. 2016.** Anthropogenic climate change drives
372 shift and shuffle in North Atlantic phytoplankton communities. *Proceedings of the*
373 *National Academy of Sciences, USA* **113**: 2964-2969.



-
- 374 **Beamud SG, Baffico GD, Reid B, Torres R, Gonzalez-Polo M, Pedrozo F, Diaz M. 2016.**
375 Photosynthetic performance associated with phosphorus availability in mats of
376 *Didymosphenia geminata* (Bacillariophyceae) from Patagonia (Argentina and Chile).
377 *Phycologia* **55**: 118-125.
- 378 **Beardall J, Roberts S, Raven JA. 2005.** Regulation of inorganic carbon acquisition by
379 phosphorus limitation in the green alga *Chlorella emersonii*. *Canadian Journal of*
380 *Botany* **83**: 859-864.
- 381 **Berg GM, Glibert PM, Lomas MW, Burford MA. 1997.** Organic nitrogen uptake and
382 growth by the chrysophyte *Aureococcus anophagefferens* during a brown tide event.
383 *Marine Biology* **129**: 377-387.
- 384 **Brembu T, Mühlroth A, Alipanah L, Bones AM. 2017.** The effects of phosphorus limitation
385 on carbon metabolism in diatoms. *Philosophical Transactions of the Royal Society B*
386 *Biological Sciences* **372**: 20160406.
- 387 **Bruland KW, Rue EL, Smith GJ. 2001.** Iron and macronutrients in California coastal
388 upwelling regimes: implications for diatom blooms. *Limnology and Oceanography* **46**:
389 1661-1674.
- 390 **Caemmerer SV, Farquhar GD. 1981.** Some relationships between the biochemistry of
391 photosynthesis and the gas exchange of leaves. *Planta* **153**: 376-387.
- 392 **Chen X, Gao K. 2004.** Photosynthetic utilisation of inorganic carbon and its regulation in the
393 marine diatom *Skeletonema costatum*. *Functional Plant Biology* **31**: 1027-1033.
- 394 **Chen X, Qiu CE, Shao JZ. 2006.** Evidence for K⁺-dependent HCO₃⁻ utilization in the marine
395 diatom *Phaeodactylum tricorutum*. *Plant Physiology* **141**: 731-736.



-
- 396 **Cheng W, Sims DA, Luo Y, Coleman JS, Johnson DW. 2010.** Photosynthesis, respiration,
397 and net primary production of sunflower stands in ambient and elevated atmospheric
398 CO₂ concentrations: an invariant NPP:GPP ratio? *Global Change Biology* **6**: 931-941.
- 399 **Davies AG, Sleep JA. 1989.** The photosynthetic response of nutrient-depleted dilute cultures
400 of *Skeletonema costatum* to pulses of ammonium and nitrate; the importance of
401 phosphate. *Journal of Plankton Research* **11**: 141-164.
- 402 **Dickson AG. 1990.** Standard potential of the reaction: $\text{AgCl(s)} + 12\text{H}_2\text{(g)} = \text{Ag(s)} + \text{HCl(aq)}$,
403 and the standard acidity constant of the ion HSO_4^- in synthetic sea water from 273.15
404 to 318.15 K. *Journal of Chemical Thermodynamics* **22**: 113-127.
- 405 **Falkowski P. 2012.** Ocean Science: The power of plankton. *Nature* **483**: 17-20.
- 406 **Field CB, Behrenfeld MJ, Randerson JT, Falkowski P. 1998.** Primary production of the
407 biosphere: integrating terrestrial and oceanic components. *Science* **281**: 237-240.
- 408 **Gao G, Gao K, Giordano M. 2009.** Responses to solar UV radiation of the diatom
409 *Skeletonema costatum* (Bacillariophyceae) grown at different Zn²⁺ concentrations
410 *Journal of Phycology* **45**: 119-129.
- 411 **Gao G, Liu Y, Li X, Feng Z, Xu J. 2016.** An ocean acidification acclimatised green tide alga
412 Is robust to changes of seawater carbon chemistry but vulnerable to light stress. *PLoS*
413 *One* **11**: e0169040.
- 414 **Geider RJ, Macintyre HL, Graziano LM, McKay RML. 1998.** Responses of the
415 photosynthetic apparatus of *Dunaliella tertiolecta* (Chlorophyceae) to nitrogen and
416 phosphorus limitation. *European Journal of Phycology* **33**: 315-332.
- 417 **Gifford RM. 1995.** Whole plant respiration and photosynthesis of wheat under increased CO₂



-
- 418 concentration and temperature: long-term vs. short-term distinctions for modelling.
- 419 *Global Change Biology* **1**: 385–396.
- 420 **Hansen PJ. 2002.** Effect of high pH on the growth and survival of marine phytoplankton:
- 421 implications for species succession. *Aquatic Microbial Ecology* **28**: 279-288.
- 422 **Heber U. 1974.** Metabolite exchange between chloroplasts and cytoplasm. *Annual Review of*
- 423 *Plant Physiology* **25**: 393-421.
- 424 **Hinga KR. 2002.** Effects of pH on coastal marine phytoplankton. *Marine Ecology Progress*
- 425 *Series* **238**: 281-300.
- 426 **Hopkinson BM, Dupont CL, Matsuda Y. 2016.** The physiology and genetics of CO₂
- 427 concentrating mechanisms in model diatoms. *Current Opinion in Plant Biology* **31**:
- 428 51-57.
- 429 **Hopkinson BM, Morel FMM. 2011.** Efficiency of the CO₂-concentrating mechanism of
- 430 diatoms. *Proceedings of the National Academy of Sciences, USA* **108**: 3830-3837.
- 431 **Hu H, Zhang J, Chen W. 2011.** Competition of bloom-forming marine phytoplankton at low
- 432 nutrient concentrations. *Journal of Environmental Sciences* **23**: 656-663.
- 433 **Hu H, Zhou Q. 2010.** Regulation of inorganic carbon acquisition by nitrogen and phosphorus
- 434 levels in the *Nannochloropsis* sp. *World Journal of Microbiology & Biotechnology* **26**:
- 435 957-961.
- 436 **Jeong HJ, An SL, Franks PJS, Lee KH, Ji HK, Kang NS, Lee MJ, Jang SH, Lee SY,**
- 437 **Yoon EY. 2015.** A hierarchy of conceptual models of red-tide generation: Nutrition,
- 438 behavior, and biological interactions. *Harmful Algae* **47**: 97-115.
- 439 **Jiang X, Han Q, Gao X, Gao G. 2016.** Conditions optimising on the yield of biomass, total



-
- 440 lipid, and valuable fatty acids in two strains of *Skeletonema menzeli*. *Food Chemistry*
- 441 **194**: 723-732.
- 442 **Li G, Gao K, Yuan D, Zheng Y, Yang G. 2011.** Relationship of photosynthetic carbon
- 443 fixation with environmental changes in the Jiulong River estuary of the South China
- 444 Sea, with special reference to the effects of solar UV radiation. *Marine Pollution*
- 445 *Bulletin* **62**: 1852-1858.
- 446 **Lin S, Litaker RW, Sunda WG. 2016.** Phosphorus physiological ecology and molecular
- 447 mechanisms in marine phytoplankton. *Journal of Phycology* **52**: 10.
- 448 **Liu Y, Song X, Cao X, Yu Z. 2012.** Responses of photosynthetic characters of *Skeletonema*
- 449 *costatum* to different nutrient conditions. *Journal of Plankton Research* **35**: 165-176.
- 450 **Maberly SC. 1990.** Exogenous sources of inorganic carbon for photosynthesis by marine
- 451 macroalgae. *Journal of Phycology* **26**: 439-449.
- 452 **Mccall SJ, Hale MS, Smith JT, Read DS, Bowes MJ. 2017.** Impacts of phosphorus
- 453 concentration and light intensity on river periphyton biomass and community structure.
- 454 *Hydrobiologia* **792**: 315-330.
- 455 **Moore CM, Mills MM, Arrigo KR, Bermanfrank I, Bopp L, Boyd PW, Galbraith ED,**
- 456 **Geider RJ, Guieu C, Jaccard SL. 2013.** Processes and patterns of oceanic nutrient
- 457 limitation. *Nature Geoscience* **6**: 701-710.
- 458 **Müller S, Mitrovic SM. 2015.** Phytoplankton co-limitation by nitrogen and phosphorus in a
- 459 shallow reservoir: progressing from the phosphorus limitation paradigm.
- 460 *Hydrobiologia* **744**: 255-269.
- 461 **Nelson DM, Tréguer P, Brzezinski MA, Leynaert A, Quéguiner B. 1995.** Production and



-
- 462 dissolution of biogenic silica in the ocean: Revised global estimates, comparison with
463 regional data and relationship to biogenic sedimentation. *Global Biogeochemical*
464 *Cycles* **9**: 359-372.
- 465 **Nimer NA, Ling MX, Brownlee C, Merrett MJ. 1999.** Inorganic carbon limitation,
466 exofacial carbonic anhydrase activity, and plasma membrane redox activity in marine
467 phytoplankton species. *Journal of Phycology* **35**: 1200-1205.
- 468 **Nimer NA, Warren M, Merrett MJ. 1998.** The regulation of photosynthetic rate and
469 activation of extracellular carbonic anhydrase under CO₂-limiting conditions in the
470 marine diatom *Skeletonema costatum*. *Plant Cell and Environment* **21**: 805–812.
- 471 **Pierrot D, Lewis E, Wallace DWR. 2006.** MS Excel program developed for CO₂ system
472 calculations. *ORNL/CDIAC-105a. Carbon Dioxide Information Analysis Center, Oak*
473 *Ridge National Laboratory, US Department of Energy, Oak Ridge, Tennessee.*
- 474 **Raven JA, Beardall J, Sánchez-Baracaldo P. 2017.** The possible evolution, and future, of
475 CO₂-concentrating mechanisms. *Journal of Experimental Botany*.
- 476 **Raven JA, Giordano M, Beardall J, Maberly SC. 2012.** Algal evolution in relation to
477 atmospheric CO₂: carboxylases, carbon-concentrating mechanisms and carbon
478 oxidation cycles. *Phil. Trans. R. Soc. B* **367**: 493-507.
- 479 **Reed ML, Pinckney JL, Keppler CJ, Brock LM, Hogan SB, Greenfield DI. 2016.** The
480 influence of nitrogen and phosphorus on phytoplankton growth and assemblage
481 composition in four coastal, southeastern USA systems. *Estuarine Coastal & Shelf*
482 *Science* **177**: 71-82.
- 483 **Rost B, Riebesell U, Burkhardt S, Sültemeyer D. 2003.** Carbon acquisition of



-
- 484 bloom-forming marine phytoplankton. *Limnology and Oceanography* **48**: 55-67.
- 485 **Roy RN, Roy LN, Vogel KM, Porter-Moore C, Pearson T, Good CE, Millero FJ,**
486 **Campbell DM. 1993.** The dissociation constants of carbonic acid in seawater at
487 salinities 5 to 45 and temperatures 0 to 45°C. *Marine Chemistry* **44**: 249-267.
- 488 **Rubinstein B, Luster DG. 1993.** Plasma membrane redox activity: components and role in
489 plant processes. *Annual Review of Plant Biology* **44**: 131-155.
- 490 **Smetacek V, Zingone A. 2013.** Green and golden seaweed tides on the rise. *Nature* **504**:
491 84-88.
- 492 **Smith NG, Dukes JS. 2013.** Plant respiration and photosynthesis in global-scale models:
493 incorporating acclimation to temperature and CO₂. *Global Change Biology* **19**: 45-63.
- 494 **Wang J. 2002.** Phytoplankton communities in three distinct ecotypes of the Changjiang
495 estuary. *Journal of Ocean University of China* **32**: 422-428.
- 496 **Wu H, Gao K. 2009.** Ultraviolet radiation stimulated activity of extracellular carbonic
497 anhydrase in the marine diatom *Skeletonema costatum*. *Functional Plant Biology* **36**:
498 137-143.
- 499 **Wu X, Gao G, Giordano M, Gao K. 2012.** Growth and photosynthesis of a diatom grown
500 under elevated CO₂ in the presence of solar UV radiation. *Fundamental and Applied*
501 *Limnology* **180**: 279-290.
- 502 **Xu Z, Gao G, Xu J, Wu H. 2017.** Physiological response of a golden tide alga (*Sargassum*
503 *muticum*) to the interaction of ocean acidification and phosphorus enrichment.
504 *Biogeosciences* **14**: 671-681.
- 505 **Young JN, Morel FMM. 2015.** Biological oceanography: The CO₂ switch in diatoms. *Nature*



506 *Climate Change* **5**: 722-723.

507 **Ziska LH, Bunce JA. 1998.** The influence of increasing growth temperature and CO₂
508 concentration on the ratio of respiration to photosynthesis in soybean seedlings.

509 *Global Change Biology* **4**: 637-643.

510 **Zou D, Gao K. 2013.** Thermal acclimation of respiration and photosynthesis in the marine
511 macroalga *Gracilaria lemaneiformis* (Gracilariales, Rhodophyta). *Journal of*
512 *Phycology* **49**: 61–68.

513



514 **Figure legends**

515 **Fig. 1.** Net photosynthetic rate (a) and dark respiration rate (b) in *S. costatum* grown at
516 various phosphate concentrations after ambient (AC) and low CO₂ (LC) treatments. The error
517 bars indicate the standard deviations (n = 3). Different letters represent the significant
518 difference ($P < 0.05$) among phosphate concentrations (capital for AC, lower case for LC).
519 Horizontal lines represent significant difference ($P < 0.05$) between CO₂ treatments.

520 **Fig. 2.** Ratio of respiration rate to net photosynthetic rate in *S. costatum* grown at various
521 phosphate concentrations after ambient (AC) and low CO₂ (LC) treatments. The error bars
522 indicate the standard deviations (n = 3). Different letters represent the significant difference (P
523 < 0.05) among phosphate concentrations (capital for AC, lower case for LC). Horizontal lines
524 represent significant difference ($P < 0.05$) between CO₂ treatments.

525 **Fig. 3.** Relative electron transport rate (rETR) in *S. costatum* grown at various phosphate
526 concentrations after ambient (AC) and low CO₂ (LC) treatments. The error bars indicate the
527 standard deviations (n = 3). Different letters represent the significant difference ($P < 0.05$)
528 among phosphate concentrations (Capital for AC lower case for LC). Horizontal lines
529 represent significant difference ($P < 0.05$) between CO₂ treatments.

530 **Fig. 4.** Photosynthetic Chl *a* content in *S. costatum* grown at various phosphate concentrations
531 after ambient (AC) and low CO₂ (LC) treatments. The error bars indicate the standard
532 deviations (n = 3). Different letters represent the significant difference ($P < 0.05$) among
533 phosphate concentrations (capital for AC, lower case for LC). Horizontal lines represent
534 significant difference ($P < 0.05$) between CO₂ treatments.

535 **Fig. 5.** Net photosynthetic rate as a function of DIC for *S. costatum* grown at various



536 phosphate concentrations after ambient (a) and low CO₂ (b) treatments. The error bars

537 indicate the standard deviations (n = 3).

538 **Fig. 6.** Half saturation constant ($K_{0.5}$) for CO₂ in *S. costatum* grown at at various phosphate

539 concentrations after ambient (AC) and low CO₂ (LC) treatments. The error bars indicate the

540 standard deviations (n = 3). Different letters represent the significant difference ($P < 0.05$)

541 among phosphate concentrations (capital for AC, lower case for LC). Horizontal lines

542 represent significant difference ($P < 0.05$) between CO₂ treatments.

543 **Fig. 7.** CA_{ext} activity (a) and reduction rate of ferricyanide (b) in *S. costatum* grown at various

544 phosphate concentrations after ambient (AC) and low CO₂ (LC) treatments. The error bars

545 indicate the standard deviations (n = 3). Different letters represent the significant difference (P

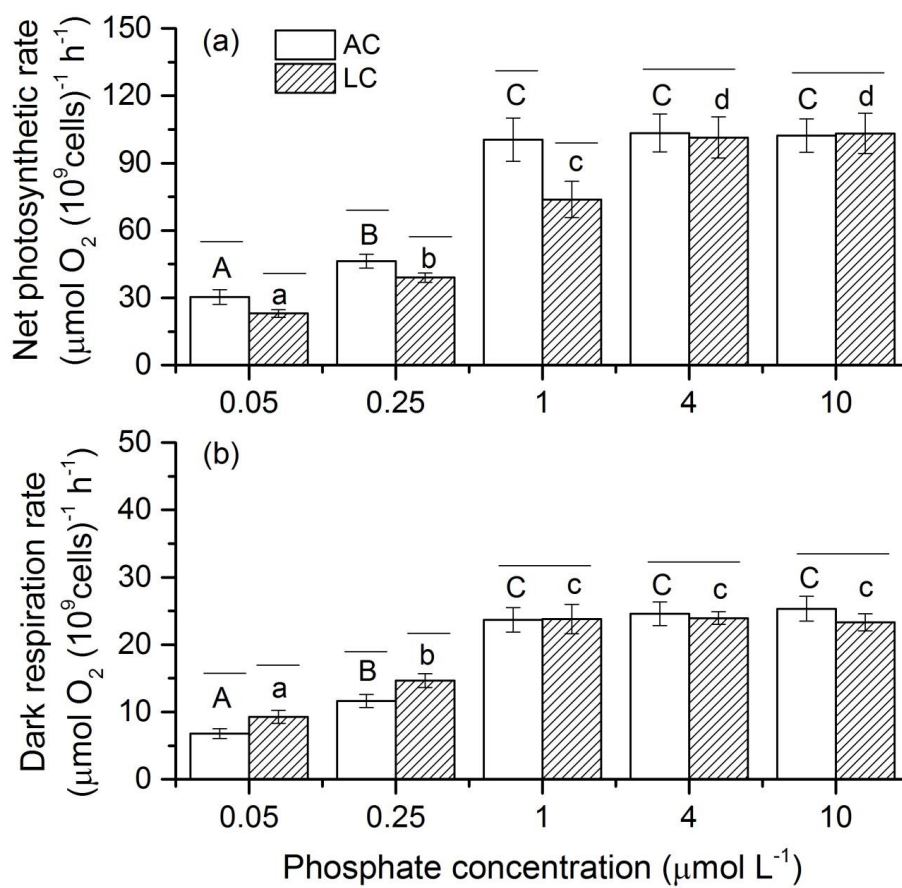
546 < 0.05) among phosphate concentrations (capital for AC, lower case for LC). Horizontal lines

547 represent significant difference ($P < 0.05$) between CO₂ treatments.

548 **Fig. 8.** Changes of pH in a closed system caused by photosynthesis of *S. costatum* grown at

549 various phosphate concentrations after ambient (AC) and low CO₂ (LC) treatments. The error

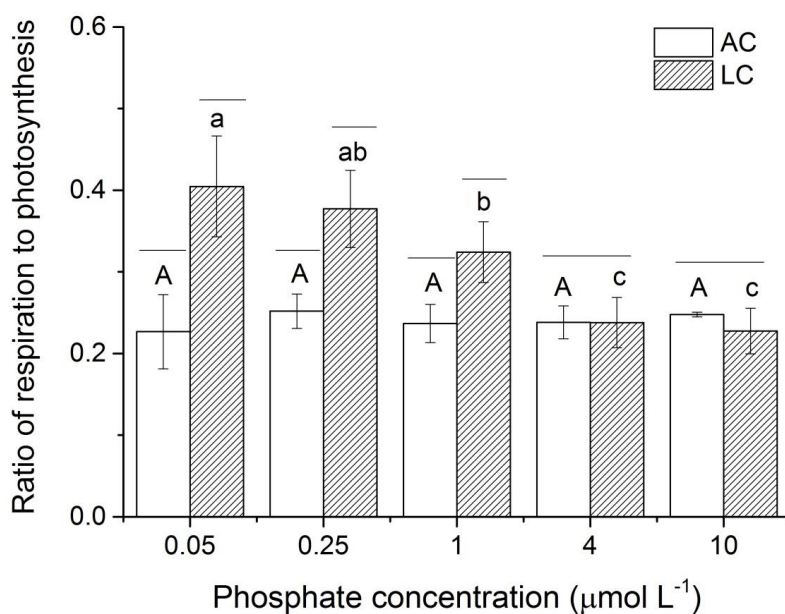
550 bars indicate the standard deviations (n = 3).



551

552

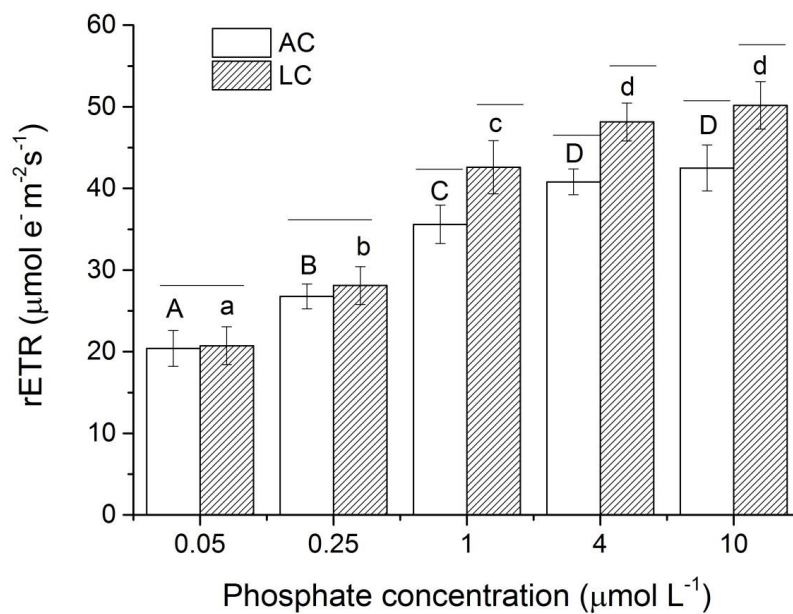
Fig. 1



553

554

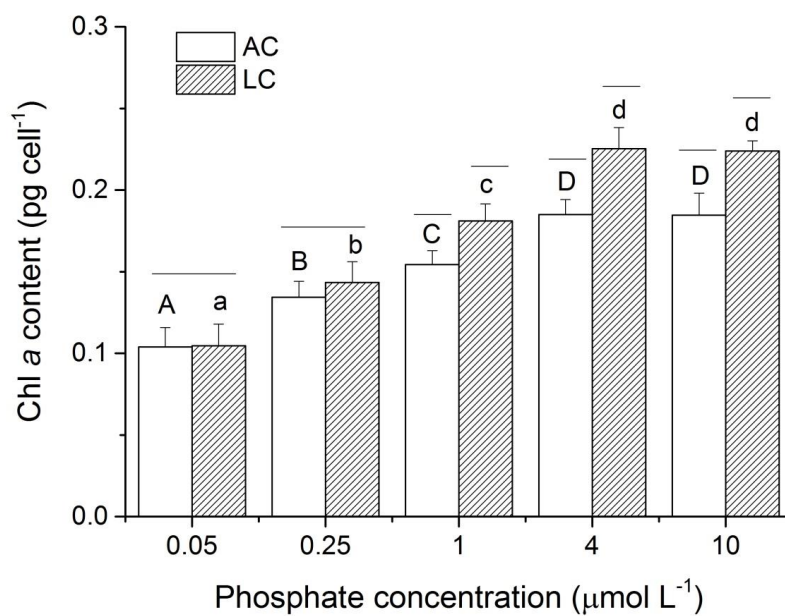
Fig. 2



555

556

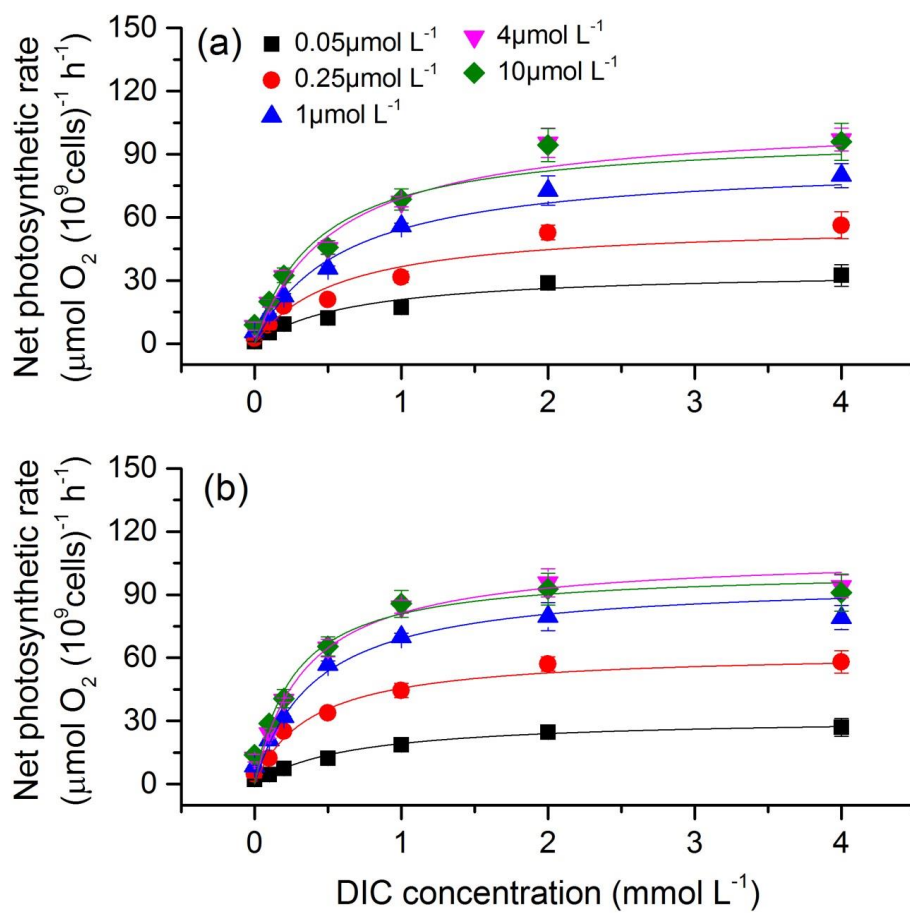
Fig. 3



557

558

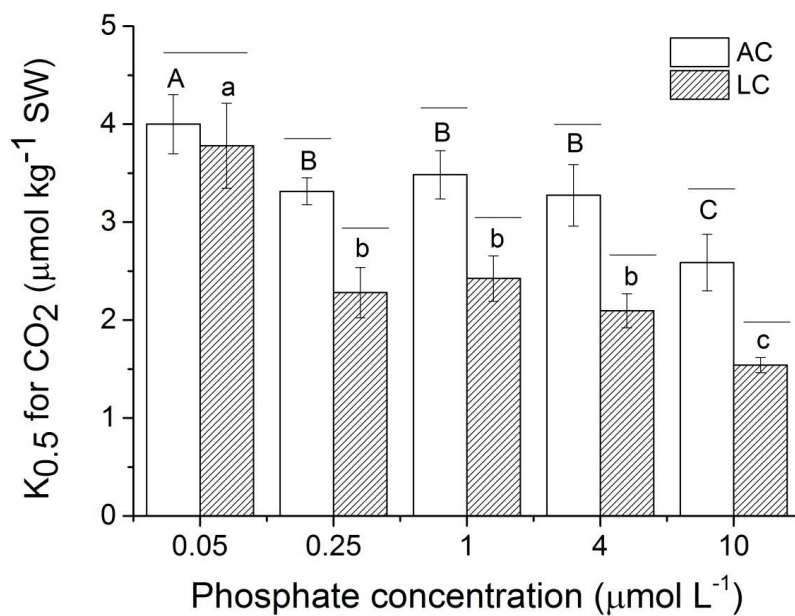
Fig. 4



559

560

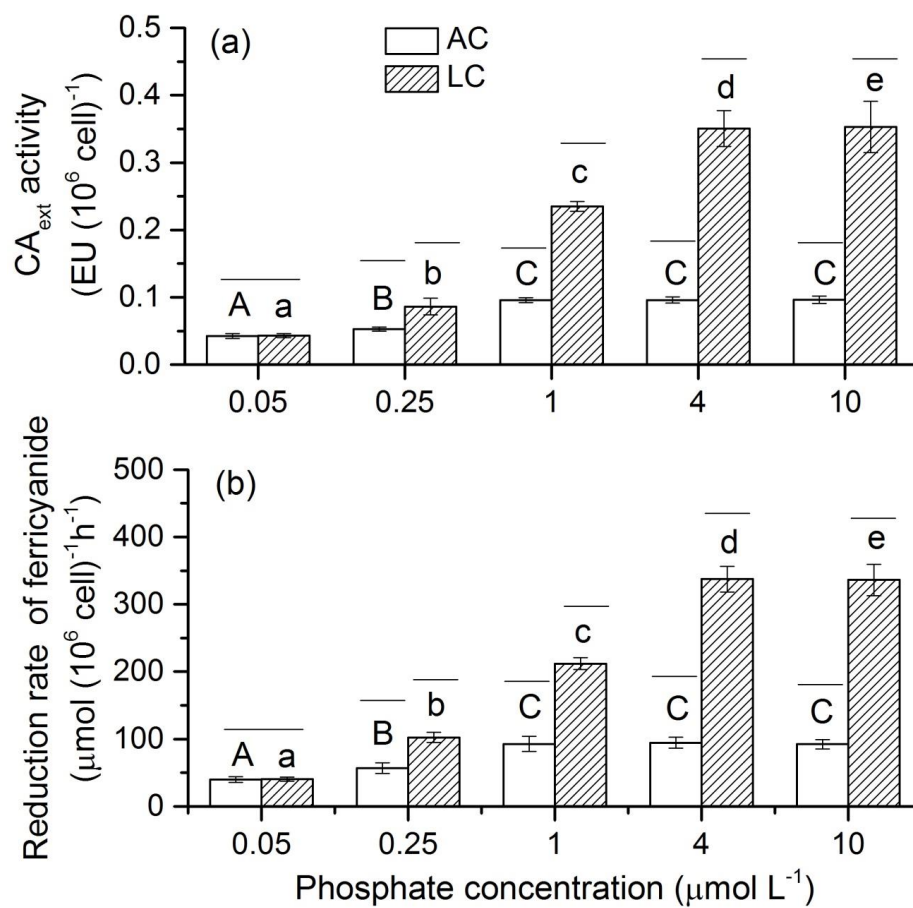
Fig. 5



561

562

Fig. 6



563

564

Fig. 7

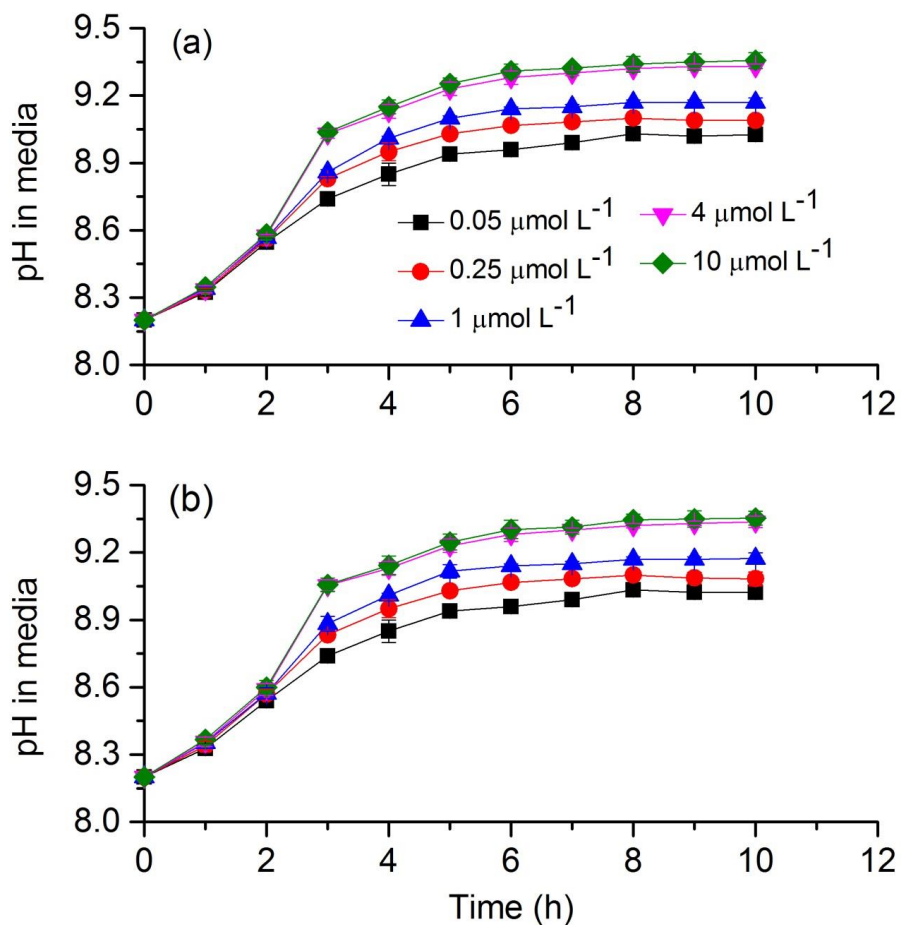


Fig. 8

565

566

567

568